

## Oxidative Lactonization of Dimethyl Ester of Chlorin $e_6$

Evgeny S. Belyaev, Vladimir S. Tyurin,<sup>@</sup> and Ilya A. Zamilatskov

*A.N. Frumkin Institute of Physical Chemistry and Electrochemistry, Russian Academy of Sciences, 119071 Moscow, Russia*

<sup>@</sup>Corresponding author E-mail: vst-1970@mail.ru

*A new transformation of the 15<sup>2</sup>,17<sup>3</sup>-dimethyl ester of chlorin  $e_6$ , leading to its 13<sup>1</sup>,13<sup>3</sup>-lactone derivative, has been discovered. The reaction proceeded at treatment of the substrate with lead tetraacetate in presence of LiCl, during which oxidative cyclization was observed leading to the formation of a lactone cycle fused with the tetrapyrrole macrocycle at positions 13 and 15. The reaction mechanism has been suggested, and quantum chemical calculations were carried out to substantiate the mechanism.*

**Keywords:** Chlorin  $e_6$ , lactone, photosensitizers, lead tetraacetate, oxidative lactonization.

## Окислительная лактонизация диметилового эфира хлорина $e_6$

Е. С. Беляев, В. С. Тюрин,<sup>@</sup> И. А. Замилацков

*Институт физической химии и электрохимии им. А.Н. Фрумкина РАН, 119071 Москва, Российская Федерация*

<sup>@</sup>E-mail: vst-1970@mail.ru

*Обнаружена новая трансформация 15<sup>2</sup>,17<sup>3</sup>-диметилового эфира хлорина  $e_6$ , приводящая к его 13<sup>1</sup>,13<sup>3</sup>-лактонному производному. Реакция протекает при обработке субстрата тетраацетатом свинца в присутствии LiCl, в ходе которой происходит окислительная циклизация с образованием лактонного цикла, сочлененного с тетрапиррольным макроциклом в 13 и 15 положениях. Предложен механизм реакции, проведены квантово-химические расчеты для обоснования механизма.*

**Ключевые слова:** Хлорин  $e_6$ , лактон, фотосенсибилизаторы, тетраацетат свинца, окислительная лактонизация.

### Introduction

Tetrapyrrole compounds are increasingly used in a wide variety of applications.<sup>[1]</sup> A large proportion of these compounds are derivatives of natural porphyrins and chlorins. The asymmetric substitution of the tetrapyrrole macrocycle of natural chlorins by several functional groups is responsible for their unique properties. Further transformations of substituents in the macrocycle make it possible to tune the molecule for specific applications, in particular, for the creation of highly effective photosensitizers for photodynamic therapy (PDT).<sup>[2-5]</sup> In particular, the transformation products of chlorophyll *a* and its derivatives (pheophorbide *a*, chlorin  $e_6$ ) contain unsaturated, aromatic, ester and other electron-active groups. The presence of three carboxyl groups of different properties and reactivity in the chlorin  $e_6$  and their ability to be selectively transformed make it easy to vary the structure and

properties of the corresponding tetrapyrrole derivatives.<sup>[6,7]</sup> Several second-generation photosensitizers for PDT have been developed based on chlorin  $e_6$ : L-aspartyl amide derivative of the 15-carboxymethyl substituent of the chlorin  $e_6$  is known as Talaporfin,<sup>[8]</sup> trisodium salt and dimeglumine sodium salt of the chlorin  $e_6$  are used in therapy as Fotoran  $e_6$  and Fotoditazin, correspondingly.<sup>[9]</sup>

The classical reactions of conversion of chlorophyll *a* into well-known derivatives have been well studied. However, the search for possible transformations has not been exhausted, and new works are constantly published, reporting the synthesis of new derivatives and their investigation as photosensitizers for PDT.<sup>[10]</sup> Lactone derivatives of chlorins are especially valuable, as the lactone moiety represents pharmaceutical, biological, and medicinal interest.<sup>[11, 12]</sup>

This work is a part of our studies of methods of functionalization of porphyrins and chlorins aimed to

preparation of photosensitizers for PDT. In particular, creation of the additional carbocycles fused with tetrapyrrole macrocycle was reported, and here a fused lactone cycle was obtained. Previously, a work has been published reporting the synthesis of a number of chlorophyll *a* derivatives based on the methyl pheophorbide *a* and transformations of substituents at 13,15 positions.<sup>[13]</sup> Some of them led to the creation of the cycles fused with tetrapyrrole macrocycle. In particular, lactone derivative of the chlorin *e*<sub>6</sub> was obtained. In the framework of this work, various transformations of chlorin *e*<sub>6</sub> were studied and the lactone derivative was obtained by an alternative way.

## Experimental

### General

Reactions were carried out under argon atmosphere using commercially available reagents that were purchased and used as received. Heating reaction vessels was performed with oil bath. Silica gel 40/60 was used for column and flash chromatography. Preparative thin layer chromatography was performed using glass plates coated with 5–40 μm silica gel (5 mm thick). <sup>1</sup>H and <sup>13</sup>C NMR spectra were recorded with a Bruker Avance III 600 MHz spectrometer at 303K in CDCl<sub>3</sub>. Chemical shifts are reported relative to signals of residual protons and carbon of solvent (CDCl<sub>3</sub> – 7.26 ppm in <sup>1</sup>H NMR, 77.16 ppm in <sup>13</sup>C NMR). The assignment of peaks in NMR spectra was done using 2D NMR techniques (COSY, HSQC). The SALDI mass-spectra were obtained on a Ultraflex-II mass spectrometer (Bruker Daltonics) in a positive ion mode using reflection mode (20 kV target voltage) without matrix. Electronic absorption spectra were recorded with U-2900 (Hitachi) spectrophotometer in quartz rectangular cells of 10 mm path length.

### Synthesis

Methyl pheophorbide *a* was obtained from commercial sources. 15<sup>2</sup>,17<sup>3</sup>-Dimethyl ester of the chlorin *e*<sub>6</sub> **1** was synthesized from the methyl pyropheophorbide *a* according to the published procedures.<sup>[14]</sup>

13<sup>1</sup>,13<sup>3</sup>-Lactone derivative of the 15<sup>2</sup>,17<sup>3</sup>-dimethyl ester of chlorin *e*<sub>6</sub> (**3**). 15<sup>2</sup>,17<sup>3</sup>-Dimethyl ester of chlorin *e*<sub>6</sub> **1** (19 mg, 0.03 mmol) was dissolved in 1,4-dioxane (2 mL), then the solution of Pb(OAc)<sub>4</sub> (62 mg, 0.14 mmol) in 1,4-dioxane (1 mL) and LiCl (2 mg, 0.048 mmol) were added and the mixture was stirred for 30 min at 80 °C. After that the reaction mixture was poured into cold water (20 mL) and extracted with CH<sub>2</sub>Cl<sub>2</sub> (2×10 mL), organic phase was washed with water (2×10 mL), dried over Na<sub>2</sub>SO<sub>4</sub>, evaporated in vacuum, and the residue was purified by flash chromatography on silica with CH<sub>2</sub>Cl<sub>2</sub>/EtOH 20:1, to give 9 mg (47%) of the product **3** as a mixture of diastereomers in a ratio of 11:10. The diastereomers were separated using preparative TLC with CH<sub>2</sub>Cl<sub>2</sub>/EtOH 25:1, yielding 5 mg (26 %) of the first diastereomer (**3a**) and 4 mg (21%) of the second diastereomer (**3b**).

**3a**: R<sub>f</sub> = 0.49 (CH<sub>2</sub>Cl<sub>2</sub>/EtOH 25:1). <sup>1</sup>H NMR (CDCl<sub>3</sub>, 303 K) δ<sub>H</sub> ppm: 9.62 (1H, s, 10-H), 9.42 (1H, s, 5-H), 8.54 (1H, s, 20-H), 7.99 (1H, dd, *J* = 17.8 Hz, *J* = 11.4 Hz, 3<sup>1</sup>-H), 7.23 (1H, s, 13<sup>3</sup>-H), 6.33 (1H, dd, *J* = 17.8 Hz, *J* = 1.2 Hz, 3<sup>2</sup>-H<sup>a</sup>), 6.19 (1H, dd, *J* = 11.4 Hz, *J* = 1.2 Hz, 3<sup>2</sup>-H<sup>b</sup>), 4.58 (1H, m, 17-H), 4.50 (1H, m, 18-H), 3.81 (3H, s, 2<sup>1</sup>-CH<sub>3</sub>), 3.72 (2H, q, *J* = 7.7 Hz, 8<sup>1</sup>-CH<sub>2</sub>), 3.60 (3H, s, 17<sup>5</sup>-CH<sub>3</sub>), 3.57 (3H, s, 13<sup>6</sup>-CH<sub>3</sub>), 3.41 (3H, s, 12<sup>1</sup>-CH<sub>3</sub>), 3.25 (3H, s, 7<sup>1</sup>-CH<sub>3</sub>), 2.66 (1H, m, 17<sup>1</sup>-CH<sub>2</sub><sup>a</sup>), 2.50 (1H, m, 17<sup>2</sup>-CH<sub>2</sub><sup>b</sup>), 2.33 (1H, m, 17<sup>1</sup>-CH<sub>2</sub><sup>b</sup>), 2.06 (1H, m, 17<sup>2</sup>-CH<sub>2</sub><sup>b</sup>), 1.71 (3H, t, *J* = 7.7 Hz, 8<sup>2</sup>-CH<sub>3</sub>), 1.61 (3H, d, *J* = 7.3 Hz, 18<sup>1</sup>-CH<sub>3</sub>), -0.54 and -0.86 (2H, each bs, NH × 2). <sup>13</sup>C NMR (CDCl<sub>3</sub>, 303 K) δ<sub>C</sub>

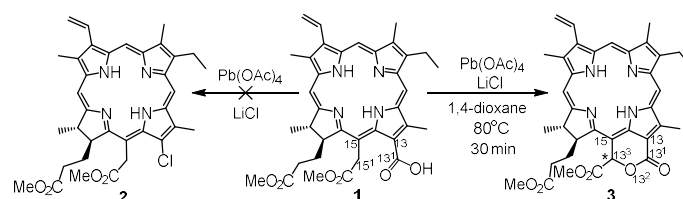
ppm: 173.5 (C17<sup>3</sup>), 172.6 (C19), 170.3 (C13<sup>4</sup>), 163.4 (C15), 162.4 (C16), 155.9 (C6), 150.0 (C9), 145.6 (C8), 142.2 (C11), 137.3 (C3), 136.4 (C4 and C12), 136.3 (C7), 134.7 (C14), 131.6 (C1), 131.5 (C2), 129.0 (C3<sup>1</sup>), 122.7 (C3<sup>2</sup>), 113.3 (C13), 104.8 (C10), 99.1 (C5), 98.9 (C13<sup>1</sup>), 93.2 (C20), 79.1 (C13<sup>3</sup>), 53.1 (C13<sup>6</sup>), 52.6 (C17), 51.6 (C17<sup>5</sup>), 50.6 (C18), 30.6 (C17<sup>1</sup> and C17<sup>2</sup>), 22.4 (C18<sup>1</sup>), 19.5 (C8<sup>1</sup>), 17.5 (C8<sup>2</sup>), 12.3 (C2<sup>1</sup>), 12.0 (C12<sup>1</sup>), 11.2 (C7<sup>1</sup>). SALDI *m/z*: found 623.29, calc. for [M+H]<sup>+</sup> C<sub>36</sub>H<sub>39</sub>N<sub>4</sub>O<sub>6</sub>: 623.2864. UV-vis (CH<sub>2</sub>Cl<sub>2</sub>) λ<sub>max</sub> (A<sub>rel.</sub>) nm: 405 (1.00), 461 (0.19), 502 (0.11), 534 (0.09), 613 (0.06), 669 (0.32).

**3b**: R<sub>f</sub> = 0.44 (CH<sub>2</sub>Cl<sub>2</sub>/EtOH 25:1). <sup>1</sup>H NMR (CDCl<sub>3</sub>, 303 K) δ<sub>H</sub> ppm: 9.76 (1H, s, 10-H), 9.59 (1H, s, 5-H), 8.76 (1H, s, 20-H), 8.06 (1H, dd, *J* = 11.6 Hz, *J* = 18.2 Hz, 3<sup>1</sup>-H), 7.52 (1H, s, 13<sup>3</sup>-H), 6.36 (1H, d, *J* = 18.2 Hz, 3<sup>2</sup>-H<sup>a</sup>), 6.22 (1H, d, *J* = 11.6 Hz, 3<sup>2</sup>-H<sup>b</sup>), 4.92 (1H, m, 17-H), 4.52 (1H, m, 18-H), 3.93 (3H, s, 2<sup>1</sup>-CH<sub>3</sub>), 3.78 (2H, q, *J* = 7.8 Hz, 8<sup>1</sup>-CH<sub>2</sub>), 3.74 (3H, s, 13<sup>6</sup>-CH<sub>3</sub>), 3.55 (3H, s, 17<sup>5</sup>-CH<sub>3</sub>), 3.48 (3H, s, 12<sup>1</sup>-CH<sub>3</sub>), 3.31 (3H, s, 7<sup>1</sup>-CH<sub>3</sub>), 2.73 (1H, m, 17<sup>1</sup>-CH<sub>2</sub><sup>a</sup>), 2.64 (1H, m, 17<sup>2</sup>-CH<sub>2</sub><sup>b</sup>), 2.42 (1H, m, 17<sup>1</sup>-CH<sub>2</sub><sup>b</sup>), 2.06 (1H, m, 17<sup>2</sup>-CH<sub>2</sub><sup>b</sup>), 1.79 (3H, d, *J* = 7.5 Hz, 18<sup>1</sup>-CH<sub>3</sub>), 1.74 (3H, t, *J* = 7.8 Hz, 8<sup>2</sup>-CH<sub>3</sub>), -1.06 and -1.66 (2H, each bs, NH × 2). <sup>13</sup>C NMR (CDCl<sub>3</sub>, 303 K) δ<sub>C</sub> ppm: 173.4 (C17<sup>3</sup>), 172.2 (C19), 170.9 (C13<sup>4</sup>), 164.8 (C15), 163.4 (C16), 155.4 (C6), 150.4 (C9), 145.5 (C8), 141.4 (C11), 138.2 (C3), 136.5 (C4), 136.1 (C12), 135.8 (C7), 133.9 (C14), 131.7 (C1), 131.2 (C2), 129.1 (C3<sup>1</sup>), 122.7 (C3<sup>2</sup>), 113.0 (C13), 103.8 (C10), 99.3 (C5), 98.6 (C13<sup>1</sup>), 93.7 (C20), 78.8 (C13<sup>3</sup>), 52.7 (C17<sup>5</sup>), 51.8 (C13<sup>6</sup>), 50.6 (C17), 49.4 (C18), 31.2 (C17<sup>1</sup>), 31.1 (C17<sup>2</sup>), 23.6 (C18<sup>1</sup>), 19.6 (C8<sup>1</sup>), 17.5 (C8<sup>2</sup>), 12.4 (C2<sup>1</sup>), 12.1 (C12<sup>1</sup>), 11.3 (C7<sup>1</sup>). SALDI *m/z*: found 623.29, calc. for [M+H]<sup>+</sup> C<sub>36</sub>H<sub>39</sub>N<sub>4</sub>O<sub>6</sub>: 623.2864. UV-vis (CH<sub>2</sub>Cl<sub>2</sub>) λ<sub>max</sub> (A<sub>rel.</sub>) nm: 405 (1.00), 461(0.19), 502 (0.11), 534 (0.09), 613 (0.06), 669 (0.32).

### Quantum-chemical calculations

Quantum-chemical calculations of geometry and electronic structure were made with the software package Gaussian 09W<sup>[15]</sup> using density functional theory (DFT) method with the hybrid correlation-exchange functional B3LYP. A full-electron 6-31G(d,p) basis set was used for the geometry optimizations, electrons of nickel and palladium atoms were rendered by the basis set with an effective potential for internal electrons LaNL2DZ. The molecules were calculated in the 1,4-dioxane solution using the polarized continuum (PCM) model. The geometry of all studied molecules was fully optimized. After the procedure of optimization of geometrical parameters wave function stability tests were carried out, then calculation of thermochemical parameters was performed. The absence of imaginary frequencies confirmed the stationary character of the optimized geometry. The energies of the calculated compounds were corrected for zero vibrational energy (ZPVE) and with thermal corrections to enthalpy and free energy were calculated at normal conditions (278.15 K, 1 atm).

Additional materials, NMR spectra and results of the DFT calculations can be found in the Electronic Supplementary Information.



**Scheme 1.** Interaction of the 15<sup>2</sup>,17<sup>3</sup>-dimethyl ester of chlorin *e*<sub>6</sub> with lead tetraacetate.

## Results and Discussion

### Synthesis

Various transformations of derivatives of both natural and synthetic porphyrins and chlorins are studied in our group targeting at preparation of new photosensitizers.<sup>[5]</sup> On the way to this, functionalization of tetrapyrrole macrocycle in order to create building blocks for palladium catalyzed cross-coupling reactions are developed.<sup>[16,17]</sup> In particular, an insertion of halogen atoms into chlorophyll *a* derivatives is studied. Insertion of bromine into pyropheophorbide *a* has been accomplished.<sup>[18]</sup> Insertion of a chlorine atom into the 15<sup>2</sup>,17<sup>3</sup>-dimethyl ester of chlorin *e*<sub>6</sub> was planned in the current work. The dimethyl ester of chlorin *e*<sub>6</sub> **1** was obtained via partial esterification of the chlorin *e*<sub>6</sub>, which was formed by hydrolysis of the corresponding trimethyl ester of chlorin *e*<sub>6</sub>. The latter was synthesized from methyl pheophorbide *a* via isocyclic ring-opening reaction being a reversed-Dieckmann condensation.<sup>[14]</sup> Initially, we attempted to replace the free 13-carboxyl group with a chlorine atom using the Kochi reaction, being a modification of the Borodin-Hunsdiecker reaction.<sup>[19]</sup> The dimethyl ester of chlorin *e*<sub>6</sub> **1** was dissolved in 1,4-dioxane and lead tetraacetate and lithium chloride were added. After 30 min of stirring at 80 °C, the initial chlorin completely disappeared and two products were formed. However, 13-chloro derivative **2** was not found among the products. Instead, the product **3** of oxidative lactonization was formed as a mixture of two diastereomers differing in the configuration of the 13<sup>3</sup>-C atom (Scheme 1) in a ratio 10:11. The diastereomers **3a** and **3b** were isolated using preparative TLC.

### Spectra

In the NMR spectrum of the product **3**, a characteristic peak of 13<sup>3</sup>-CH was observed in the form of a singlet at 7.27 ppm for the major diastereomer **3a** and 7.52 ppm for the minor diastereomer **3b**. Compared with the spectrum of the initial chlorin **1**, the peak of 15<sup>1</sup>-CH<sub>2</sub> in the form of two doublets at 5.23 and 5.50 ppm with a geminal constant of 18.6 Hz disappeared. The shift of the 13<sup>3</sup>-CH signal into a low field by 2 ppm was due to the influence of the oxygen substituent that has been attached. The remaining signals in the product spectrum correspond to the similar peaks in the original spectrum. In the <sup>13</sup>C NMR spectrum of the product the peak at 79 ppm was observed, while the carbon spectrum of the starting chlorin *e*<sub>6</sub> did not contain any signals in the region from just up 50 to over 100 ppm. The signal at 79 ppm belongs to the 13<sup>3</sup>-CH, as it was confirmed by HSQC. The main bands in the UV-vis spectrum of the product slightly changed: both the short wavelength Soret band and the longest-wavelength Q<sub>y</sub> band were bathochromically shifted by 2 and 5 nm, correspondingly, weaker Q-bands were similarly shifted. However, a new relatively intense band at 461 nm arose.

### Mechanism

We have proposed a mechanism for the reaction of oxidative cyclization of chlorin **1** into lactone **3**, and quantum chemical calculations have been carried out to confirm it. In accordance with similar reactions of lead tetraacetate

and carboxylic acids, the corresponding mixed salt of lead(IV) acetate and carboxylic acid **4** was formed at the first stage, besides that, at presence of LiCl the corresponding anion complex **5** can also be formed (Scheme 2).<sup>[20]</sup> Pb(OAc)<sub>4</sub> can also act as a Lewis acid, promoting enolization of 15-(methyl acetate) group (Scheme 3).

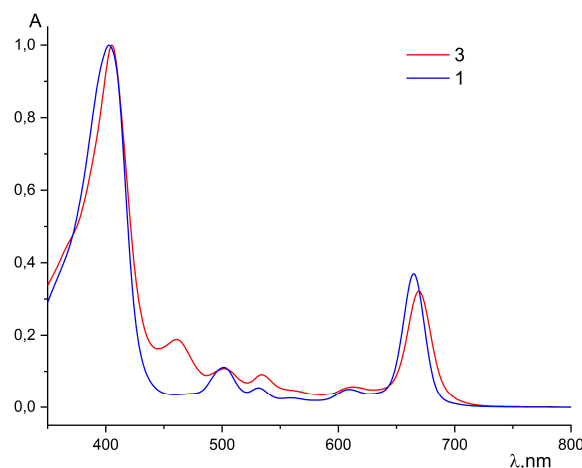
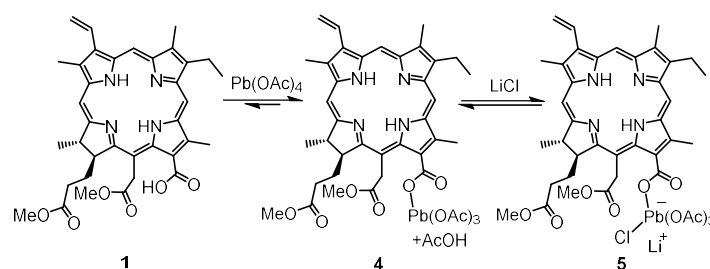
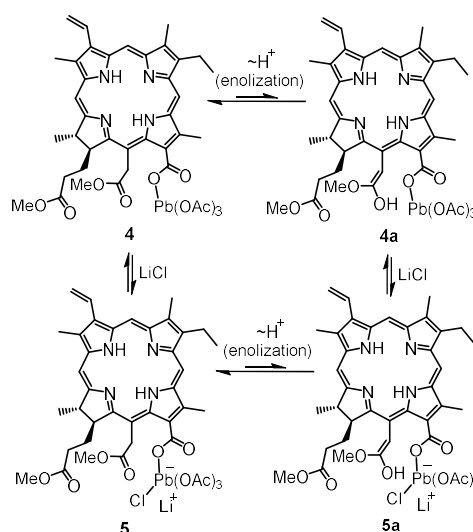


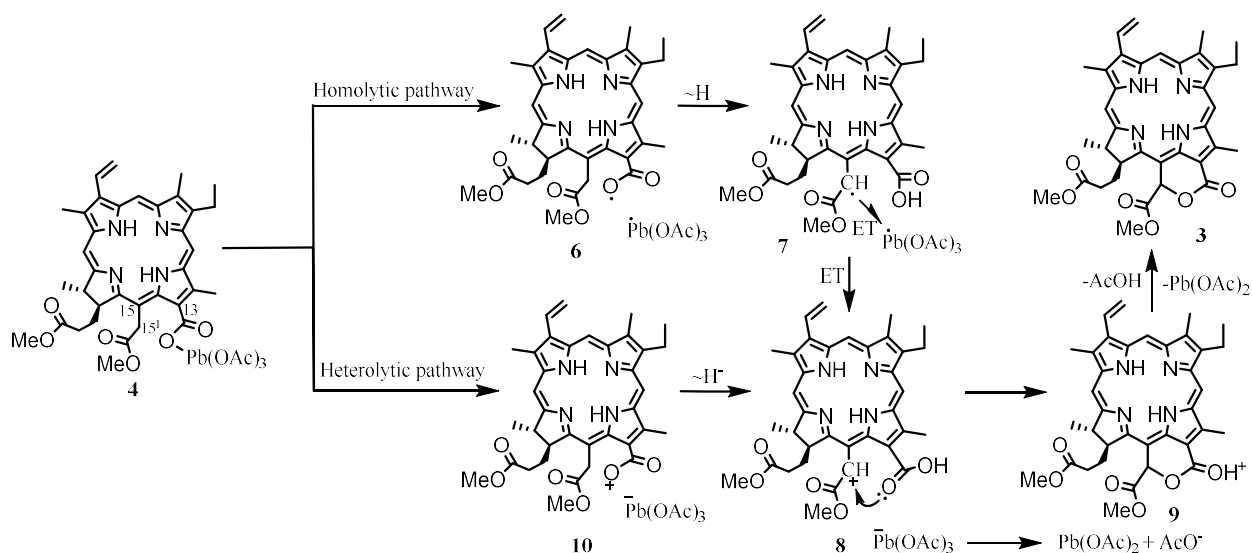
**Figure 1.** UV-vis absorption spectra of the 15<sup>2</sup>,17<sup>3</sup>-dimethyl ester of chlorin *e*<sub>6</sub> **1** and its lactone derivative **3**. Spectra were recorded in CH<sub>2</sub>Cl<sub>2</sub> at concentration of 10<sup>-5</sup> M.



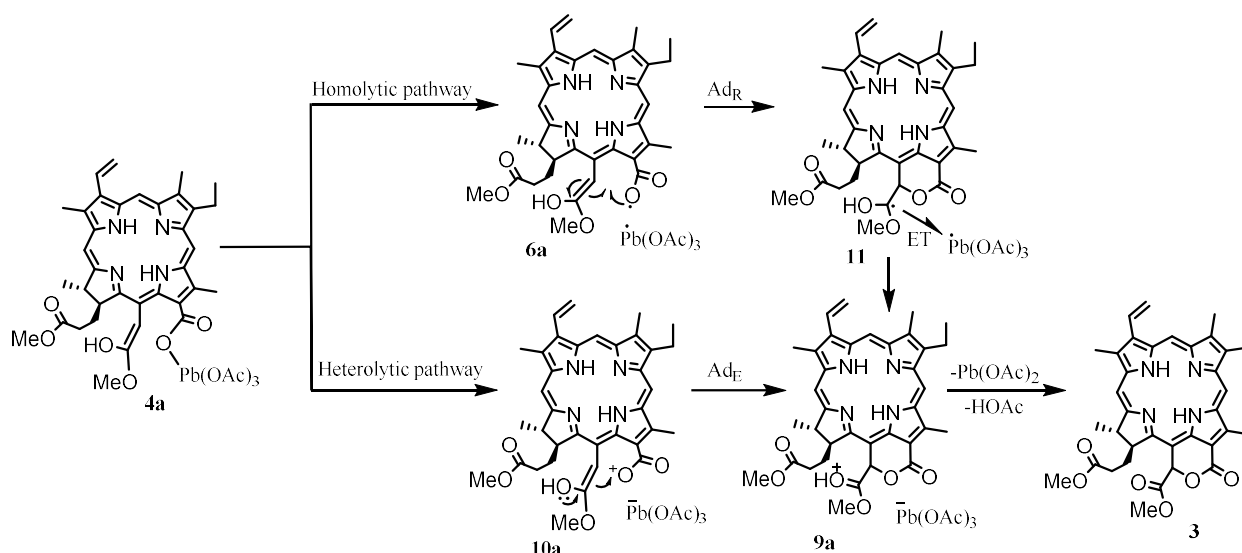
**Scheme 2.** The pre-equilibrium of the 15<sup>2</sup>,17<sup>3</sup>-dimethyl ester of chlorin *e*<sub>6</sub> **1** with lead tetraacetate and LiCl.



**Scheme 3.** Enolization of the 15-(methyl acetate) group in the lead acetate salt of the dimethyl ester of chlorin *e*<sub>6</sub>.



**Scheme 4.** Alternative pathways of the transformation of the  $Pb(OAc)_3$  salt of the dimethyl ester of chlorin  $e_6$  (4) into the lactone derivative (3).



**Scheme 5.** Alternative pathways of the transformation of the  $Pb(OAc)_3$  salt of the enol tautomer of the dimethyl ester of chlorin  $e_6$  (4a) into the lactone derivative (3).

The probable mechanism can in principle be both homolytic and heterolytic in nature, and the reaction can proceed either from the carbonyl form 4 (Scheme 4) or from the enol tautomer 4a (Scheme 5).

The Kochi reaction was shown to proceed via the radical pathway.<sup>[20,21]</sup> The homolytic decomposition of the Pb-O bond was reported to proceed faster in the anion complex of Pb(IV) compared to the neutral lead(IV) carboxylate, which is reasonably stable, and its decomposition was shown to be catalyzed by nucleophiles such as pyridine, acetate anion etc.<sup>[21]</sup> The limiting stage of the reaction is the breaking of the Pb-O bond, which in the case of the starting anionic lead complex 5 leads to an intermediate 6 with a radical center at the oxygen atom of the carboxyl group at position 13 (Scheme 6). Usually, such radicals are unstable and release a carbon dioxide molecule, resulting in a carbon radical. In the case of the alkylcarboxylic acids the

decarboxylation is very fast, as the corresponding rate constant  $k \sim 10^9 \text{ s}^{-1}$ .<sup>[22]</sup> The decarboxylation of aryl carboxylic radical is much slower with the rate constant  $k \sim 10^6 \text{ s}^{-1}$ .<sup>[23]</sup> However, the low activation barrier (8–9 kcal/mol)<sup>[23]</sup> of the decarboxylation of an aryl carboxylic radical makes need for the even lower activation energy of the desirable next reaction step of aryl carboxyl radical, which should be fast enough to promote the reaction toward the expected pathway. In our case, the carboxyl radical is aromatic. The rates of the hydrogen atom transfer (HAT) and radical addition to the carbon-carbon double bond ( $Ad_R$ ) are of the same order of  $k \sim 10^7 \text{ M}^{-1} \text{ s}^{-1}$ .<sup>[22]</sup> Thus, both the hydrogen abstraction and addition to the C=C double bond can proceed faster than the decarboxylation. Due to the spatial proximity of 15<sup>1</sup>-C to the oxygen atom of the 13-carboxyl group, after the homolytic breakup of the Pb-O bond, the resulting oxygen radical can abstract the hydrogen atom

from  $15^1\text{-CH}_2$ , forming intermediate **7**. Then the electron transfer (ET) from the  $15^1\text{-CH}$  radical center to the lead(III) triacetate leads to formation of  $15^1\text{-CH}$  carbocation in **8**. Cyclization takes place by the nucleophilic attack of the oxygen atom of the 13-carboxyl group to the  $15^1\text{-CH}$  carbocation (Scheme 6).

The similar type of lactonization was reported for 2-benzylbenzoic acids and 2-phenethyl benzoic acid using electrochemical oxidation of the benzoic acid to the corresponding radical.<sup>[24]</sup> The authors also proposed the mechanism with the analogous steps including benzylic hydrogen abstraction by the carboxylic radical, followed by the oxidation of the benzylic radical and the final cyclization step by the nucleophilic attack of the carboxylic oxygen to the benzylic cation. The radical trapping and kinetic isotopic effect confirmed the proposed mechanism. However, unlike the lactonization of the ortho-substituted benzoic acids, in the reaction of chlorin the  $15^1\text{-CH}$  carbocation **8** is destabilized by a neighboring methoxycarbonyl group. An alternative mechanism is based on the oxygen radical addition ( $\text{Ad}_\text{R}$ ) to the carbon-carbon double bond of the enol form of the dimethyl ester of chlorin  $e_6$  (Scheme 5). The methyl acetate substituent at position 15 is able to enolize under catalysis of Lewis acid  $\text{Pb}(\text{OAc})_4$ , and the resulting carbon-carbon enol double bond is in its stabilizing partial conjugation with a tetrapyrrole macrocycle (Scheme 3). Moreover, the spatial proximity of  $15^1\text{-C}$  to the carboxyl group at position 13 can lead to nucleophilic assistance of the enol group to the Pb-O bond heterolytic breakup. The enol form is especially suitable for the heterolytic pathway, in which the electrophilic oxygen cation easily attacks the electron rich carbon-carbon double bond of the enol in **10a** (Scheme 5). Electrophilic addition to the double bond leads to the protonated lacton **9a**. Thus the heterolytic pathway is the shortest route to the product.

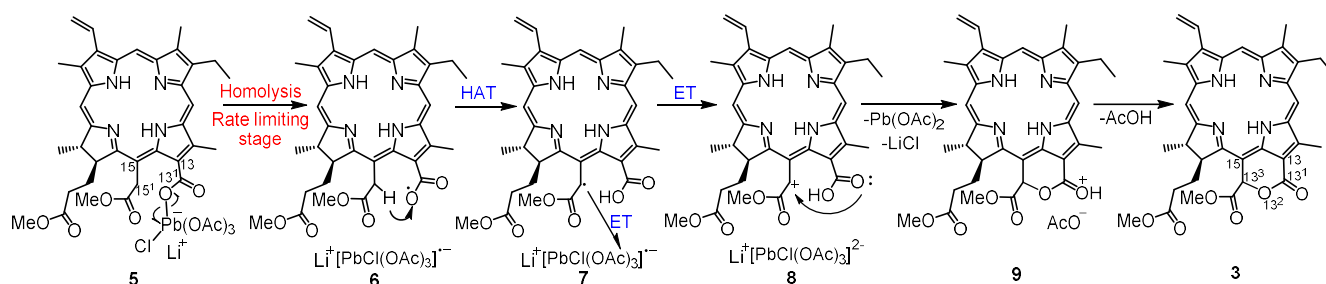
To assess the preferred nature of the reaction mechanism, we calculated the energies of the intermediates **4**, **4a**, **5** and **5a**. Quantum chemical calculations were performed using the DFT method. Optimization of the geometry of reaction species in 1,4-dioxane was performed by the B3LYP functional and 6-31G(d,p) basis set for light atoms and LanL2DZ for Pb. According to the calculations, the carbonyl form of the starting dimethyl ester of chlorin  $e_6$  **1** is more stable than the corresponding enol form **1a** by  $\sim 23$  kcal/mol, and lead acetate salt of the carbonyl form **4** is more stable than the enol **4a** by  $\sim 21$  kcal/mol (Scheme 7), so the enol pathway (Scheme 5) seems to be improbable. The formation of the lead acetate salt **4** is endothermic, so an excess of the lead tetraacetate is

needed for the equilibrium shift from **1** to **4**. But LiCl addition leads to the anionic complex formation which is energetically favorable overall ( $-7$  kcal/mol from **1** to **5**). The energy of the homolytic breakup of the Pb-O bond of **4** leading to the radical intermediate **6** was calculated to be 20 kcal/mol, and that of the heterolytic breakup leading to the cationic intermediate made up 49 kcal/mol. Thus, the energy of the homolytic breakup is 29 kcal/mol less than that of the heterolytic breakup. The Pb-O bond homolytic breakup energy of the chloride anionic complex **5** is 16 kcal/mol which is 4 kcal/mol less than that of the neutral Pb salt **4**. Thus, the DFT calculations confirmed the catalytic action of the LiCl additive in the initiation of the radical reaction. But the energy of the heterolytic Pb-O bond dissociation of the anionic complex **5**, leading to the oxygen cation formation, was calculated to be much higher than that of the neutral complex **4**, reaching a very high value of 96 kcal/mol. The dissociation of the enol form **4a** proceeds easier. The energy of the radical dissociation of the neutral salt **4a** is 18 kcal/mol, and the energy of the cation oxygen formation is 36 kcal/mol. However, this pathway does not matter due to the low equilibrium concentration of the enol tautomer. Thus, the plausible mechanism of oxidative lactonization of dimethyl chlorin  $e_6$  is homolytic and proceeds from the anionic lead(IV) complex of the dimethyl ester of chlorin  $e_6$  **5** (Scheme 6).

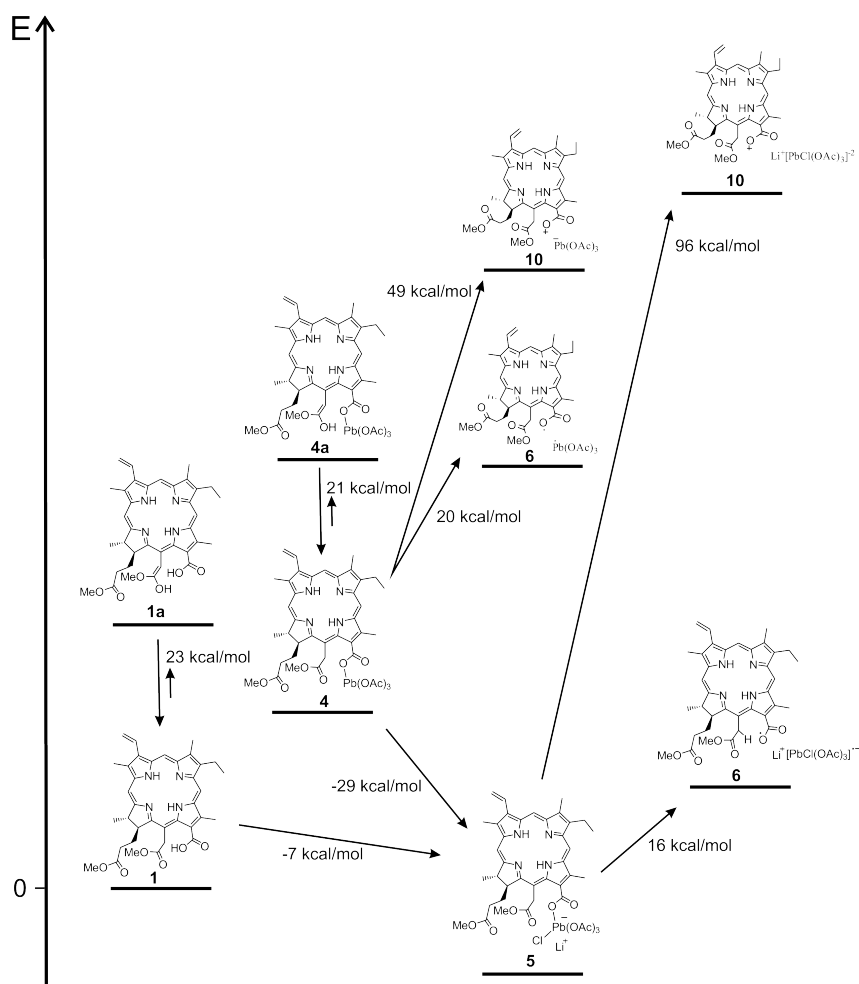
## Conclusion

In conclusion, a new transformation of the derivative of natural chlorin  $e_6$  has been discovered. As a result of the treatment of dimethyl ester of chlorin  $e_6$  with lead tetraacetate, oxidative cyclization occurs with the formation of the lactone derivative of the chlorin  $e_6$ . The quantum chemical calculation of the structures of the possible intermediates allowed to propose a plausible mechanism of the reaction. An oxidation of the substrate by lead(IV) via radical pathway leads to the carboxyl radical formation. The key step is an intramolecular hydrogen atom transfer followed by the oxidation of the radical with lead(III) through an electron transfer leading to the carbocation. Finally, the cyclization takes place by the nucleophilic attack of the oxygen atom of the carboxyl group to the carbocation. Thus, the new reaction allows to obtain the valuable derivative of chlorin  $e_6$ . The scope of the reaction is under ongoing investigation and will be reported in due course.

**Acknowledgements.** The reported study was funded by the Russian Science Foundation, grant 22-23-00903.



**Scheme 6.** The plausible mechanism of oxidative lactonization of the dimethyl ester of chlorin  $e_6$ .



**Scheme 7.** The energetic diagram of the intermediates of the oxidative lactonization of the dimethyl ester of chlorin  $e_6$ .

## References

- Shi Y., Zhang F., Linhardt R.J. *Dyes Pigment.* **2021**, *188*, 109136. DOI: 10.1016/j.dyepig.2021.109136.
- Ethirajan M., Chen Y., Joshi P., Pandey R.K. *Chem. Soc. Rev.* **2011**, *40*, 340–362. DOI: 10.1039/b915149b.
- Allison R.R., Sibata C.H. *Photodiagn. Photodyn. Ther.* **2010**, *7*(2), 61–75. DOI: 10.1016/j.pdpdt.2010.02.001.
- Glowacka-Sobotta A., Wrotynski M., Kryjewski M., Sobotta L., Mielcarek J. *J. Porphyrins Phthalocyanines* **2019**, *23*(01n02), 1–10. DOI: 10.1142/s108842461850116x.
- Koifman O.I., Ageeva T.A., Kuzmina N.S., Otvagin V.F., Nyuchev A.V., Fedorov A.Yu., Belykh D.V., Lebedeva N.Sh., Yurina E.S., Syrbu S.A., Koifman M.O., Gubarev Y.A., Bunin D.A., Gorbunova Yu.G., Martynov A.G., Tsvadze A.Yu., Dudkin S.V., Lyubimtsev A.V., Maiorova L.A., Kishalova M.V., Petrova M.V., Sheinin V.B., Tyurin V.S., Zamilatskov I.A., Zenkevich E.I., Morshnev P.K., Berezin D.B., Drondel E.A., Kustov A.V., Pogorilyy V.A., Noev A.N., Eshtukova-Shcheglova E.A., Plotnikova E.A., Plyutinskaya A.D., Morozova N.B., Pankratov A.A., Grin M.A., Abramova O.B., Kozlovitseva E.A., Drozhzhina V.V., Filonenko E.V., Kaprin A.D., Ryabova A.V., Pominova D.V., Romanishkin I.D., Makarov V.I., Loschenov V.B., Zhdanova K.A., Ivantsova A.V., Bortnevskaya Yu.S., Bragina N.A., Solovieva A.B., Kuryanova A.S., Timashev P.S. *Macroheterocycles* **2022**, *15*, 207–302. DOI: 10.6060/mhc224870k.
- van der Haas R.N.S., de Jong R.L.P., Noushazar M., Erkelens K., Smijs T.G.M., Liu Y., Gast P., Schuitmaker H.J., Lugtenburg J. *Eur. J. Org. Chem.* **2004**, *2004*, 4024–4038. DOI: 10.1002/ejoc.200400366.
- Kozyrev A.N., Chen Y., Goswami L.N., Tabaczynski W.A., Pandey R.K. *J. Org. Chem.* **2006**, *71*, 1949–1960. DOI: 10.1021/jo052334i.
- Yano T., Minamide T., Takashima K., Nakajo K., Kadota T., Yoda Y. *J. Clin. Med.* **2021**, *10*, 2785. DOI: 10.3390/jcm10132785.
- Kustov A.V., Smirnova N.L., Privalov O.A., Moryganova T.M., Strelnikov A.I., Morshnev P.K., Koifman O.I., Lyubimtsev A.V., Kustova T.V., Berezin D.B. *J. Clin. Med.* **2022**, *11*, 233. DOI: 10.3390/jcm11010233.
- Pucci C., Martinelli C., Degl'Innocenti A., Desii A., De Pasquale D., Ciofani G. *Macromol. Biosci.* **2021**, *21*, 2100181. DOI: 10.1002/mabi.202100181.
- Hur J., Jang J., Sim J. *Int. J. Mol. Sci.* **2021**, *22*, 2769. DOI: 10.3390/ijms22052769.
- Shaw S.J., Sundermann K.F., Burlingame M.A., Myles D.C., Freeze B.S., Xian M., Brouard I., Smith A.B. *J. Am. Chem. Soc.* **2005**, *127*, 6532–6533. DOI: 10.1021/ja051185i.
- Yin J., Jang W. Z., Yang Zea, Liu Chao, Zhao Lili, Wang Jinjun *Chin. J. Org. Chem.* **2012**, *32*, 360–367. DOI: 10.6023/cjoc1108301.
- Hargus J.A., Fronczek F.R., Vicente M.G.H., Smith K.M. *Photochem. Photobiol.* **2007**, *83*, 1006–1015. DOI: 10.1111/j.1751-1097.2007.00092.x.
- Frisch M.J., Trucks G.W., Schlegel H.B., Scuseria G.E., Robb M.A., Cheeseman J.R., Scalmani G., Barone V., Mennucci B., Petersson G.A., Nakatsuji H., Caricato M., Li X., Hratchian

- H.P., Izmaylov A.F., Bloino J., Zheng G., Sonnenberg J.L., Hada M., Ehara M., Toyota K., Fukuda R., Hasegawa J., Ishida M., Nakajima T., Honda Y., Kitao O., Nakai H., Vreven T., Montgomery J.A.J., Peralta J.E., Ogliaro F., Bearpark M., Heyd J.J., Brothers E., Kudin K.N., Staroverov V.N., Keith T., Kobayashi R., Normand J., Raghavachari K., Rendell A., Burant J.C., Iyengar S.S., Tomasi J., Cossi M., Rega N., Millam J.M., Klene M., Knox J.E., Cross J.B., Bakken V., Adamo C., Jaramillo J., Gomperts R., Stratmann R.E., Yazyev O., Austin A.J., Cammi R., Pomelli C., Ochterski J.W., Martin R.L., Morokuma K., Zakrzewski V.G., Voth G.A., Salvador P., Dannenberg J.J., Dapprich S., Daniels A.D., Farkas O., Foresman J.B., Ortiz J.V., Cioslowski J., Fox D.J. *Gaussian 09, Revision D.01*, Gaussian, Inc., Wallingford CT, **2013**.
16. Belyaev E.S., Kozhemyakin G.L., Tyurin V.S., Frolova V.V., Lonin I.S., Ponomarev G.V., Buryak A.K., Zamilatskov I.A. *Org. Biomol. Chem.* **2022**, *20*, 1926–1932. DOI: 10.1039/D1OB02005F.
17. Kozhemyakin G.L., Tyurin V.S., Shkirdova A.O., Belyaev E.S., Kirinova E.S., Ponomarev G.V., Chistov A.A., Aralov A.V., Tafeenko V.A., Zamilatskov I.A. *Org. Biomol. Chem.* **2021**, *19*, 9199–9210. DOI: 10.1039/D1OB01626A.
18. Lonin I.S., Kuzovlev A.S., Belyaev E.S., Ponomarev G.V., Koifman O.I., Tsivadze A.Y. *J. Porphyrins Phthalocyanines* **2014**, *18*, 123–128. DOI: 10.1142/s108842461350123x.
19. Varenikov A., Shapiro E., Gandelman M. *Chem. Rev.* **2021**, *121*, 412–484. DOI: 10.1021/acs.chemrev.0c00813.
20. Kochi J.K. *J. Org. Chem.* **1965**, *30*, 3265–3271. DOI: 10.1021/jo01021a002.
21. Kochi J.K. *J. Am. Chem. Soc.* **1965**, *87*, 2500–2502. DOI: 10.1021/ja01089a041.
22. Hu X.-Q., Liu Z.-K., Hou Y.-X., Gao Y. *iScience* **2020**, *23*(7), 101266. DOI: 10.1016/j.isci.2020.101266.
23. Chateaufneuf J., Luszyk J., Ingold K.U. *J. Am. Chem. Soc.* **1988**, *110*, 2886–2893. DOI: 10.1021/ja00217a032.
24. Zhang S., Li L., Wang H., Li Q., Liu W., Xu K., Zeng C. *Org. Lett.* **2018**, *20*, 252–255. DOI: 10.1021/acs.orglett.7b03617.

Received 11.10.2023

Accepted 29.11.2023